学 位 論 文

Effects of the expectorant drug ambroxol
hydrochloride on chemically induced lung
inflammatory and neoplastic lesions in
rodents

香川大学大学院医学系研究科
分子情報制御医学専攻

吉 田 翔 太

Original Article

Effects of the expectorant drug ambroxol hydrochloride on chemically induced lung inflammatory and neoplastic lesions in rodents

Shota Yoshida[1, 2], Masanao Yokohira[1], Keiko Yamakawa[1], Yuko Nakano-Narusawa[1], Shohei Kanie [2], Nozomi Hashimoto[1], and Katsumi Imaida[1*]

[1] Onco-Pathology, Department of Pathology and Host Defense, Faculty of Medicine, Kagawa University, 1750-1 Ikenobe, Miki-cho, Kita-gun, Kagawa 761-0793, Japan

[2] Toxicology Laboratory, Discovery and Preclinical Research Division, TAIHO Pharmaceutical Co., Ltd., 224-2 Ebisuno, Hiraishi, Kawauchi-cho, Tokushima 771-0194, Japan

Abstract: Ambroxol hydrochloride (AH) is an expectorant drug used to stimulate pulmonary surfactant and serous airway secretion. Surfactant proteins (SPs) are essential for maintaining respiratory structure and function, although SP expression has also been reported in lung inflammatory and proliferative lesions. To determine whether AH exerts modulatory effects on these lung lesions, we examined its effects on pleural thickening induced by intrathoracic administration of dipotassium titanate (TISMO) in A/JJmsSlc (A/J) mice. We also analyzed the modulatory effects of AH on neoplastic lung lesions induced by 4-(methylnitrosamino)-1-(3-pyridyl)-1-butanone (NNK) in A/J mice and by N-nitrosobis (2-hydroxypropyl) amine (DHPN) in F344/DuCrlCrj (F344) rats. A/J mice treated with TISMO showed decreased body weight, increased white blood cell (WBC) counts, and pleural thickening caused by pleuritis and poor general condition. However, A/J mice treated with TISMO + 120 ppm showed significant recovery of body weight and WBC counts to the same levels as those of A/J mice not treated with TISMO, although no significant differences were observed in histopathological changes including the immunohistopathological expression of IL-1β in the lung and maximum pleural thickness regardless of AH treatment. In the NNK and DHPN experiments, no significant differences in body weight, hematology, plasma biochemistry, and histopathological changes were associated with AH concentration. These results suggest that AH potentially exerts anti-inflammatory effects but does not have a direct suppressive effect on lung tumorigenesis in rodents. (DOI: 10.1293/tox.2018-0012; J Toxicol Pathol 2018; 31: 255–265)

Key words: ambroxol hydrochloride, lung carcinogenesis, lung inflammation, DHPN, NNK, TISMO

Introduction

Pulmonary surfactant proteins (SPs) are secreted by alveolar type II epithelial cells and Clara cells and comprise the following four subtypes: SP-A, SP-B, SP-C, and SP-D. SP-A and SP-D appear to have an essential role in host defense mechanisms, whereas SP-B and SP-C are important in lowering surface tension in the lung[1, 2].

In previous experiments, we investigated the expression of SPs in rodent neoplastic lung lesions induced by the administration of N-nitrosobis (2-hydroxypropyl) amine (DHPN) via drinking water for 2 weeks and in inflammatory lung lesions induced by a single intratracheal instillation (i.t.) of quartz, a particle known to induce lung inflammation, in male F344/DuCrlCrj (F344) rats[2, 3]. SP-A and SP-D were found to be strongly expressed in alveolar mucus and in macrophages observed in the inflammatory lung lesions[2]. In addition, SP-B and SP-C were highly detected in the bronchial/alveolar epithelial cells of the inflammatory lesions as well as in lung hyperplasias and adenomas. These results suggested that SP expression was associated with lung tumorigenesis[2].

Ambroxol hydrochloride (AH), an expectorant drug, is clinically prescribed to stimulate pulmonary surfactant and serous airway secretion, thus enhancing airway ciliary movement and facilitating sputum removal[4, 5]. AH treatment has also been reported to regulate SP production[6]. The protein and mRNA contents of SP-C increased in alveolar type-II epithelial cells from AH-treated rats. AH treatment also resulted in a significant increase in SP-B in whole lung tissue as revealed by enhanced immunostaining of Clara cells[6]. Several reports have shown that AH treatment has

suppressive effects on pulmonary inflammation and inhibits the progression of inflammation in humans and animals[6-8]. A suppressive effect of AH on quartz-induced lung inflammation was also demonstrated in our previous study[9]. Therefore, the anti-inflammatory effect of AH is expected to be associated with reduced oxidative stress or inhibition of inflammatory cytokine production[9]. However, no studies to date have examined the effects of AH on chemically induced lung tumors in rodents.

Fiber-shaped particles of dipotassium octatitanate (TISMO®) have been reported to induce pleural thickening due to chronic pleuritis when administered intrathoracically to A/JJmsSlc (A/J) mice[10]. The tobacco-specific N-nitrosamine 4-(methylnitrosamino)-1-(3-pyridyl)-1-butanone (NNK) is considered to play important roles in tobacco-related human lung cancer[11, 12]. NNK is also a strong lung carcinogen in rodents[13]. In the mouse, it is well known that females are generally more sensitive to chemical lung carcinogenesis, such as that induced by NNK, than males[14]. Kras mutations, equivalent to human non-small cell lung cancer (NSCLC) in tobacco-smoking patients, have been detected at a high frequency in NNK-induced lung tumors[15-19]. DHPN has been reported to activate Kras gene mutations at codon 12, which are detected in almost 50% of rat lung neoplastic lesions induced by other carcinogens, e.g., NNK or MeIQx[19]. Thus, male F344 rats treated with 0.1% DHPN in drinking water for 2 weeks are commonly used as a model of lung carcinogenesis[3, 20, 21].

In the present study, three experiments were conducted to examine the additional effects of AH on chemically induced lung inflammatory and neoplastic lesions in rodents. In experiment 1, the effects of AH on pleural thickening induced by TISMO were examined in A/J mice. In experiment 2, the modulatory effects of AH were evaluated in proliferative lung lesions in A/J mice induced by NNK. In experiment 3, the effects of AH on F344 rats induced by DHPN were evaluated.

Materials and Methods

Chemicals

AH was purchased from Tokyo Chemical Industry Co., Ltd. (Tokyo, Japan). Dipotassium octatitanate fibers (TISMO-D; chemical formula $K_2O \cdot 6TiO_2$) were produced by Otsuka Chemical Co. Ltd. (Osaka, Japan) as fibers with a length (mean dimension) <50 µm and width <2 µm. For administration, the fibers were suspended in saline (isotonic sodium chloride solution; Otsuka Pharmaceutical Factory, Inc., Tokushima, Japan). The suspension in saline showed both aggregated TISMO fibers as well as separated single fibers[22]. NNK was purchased from Toronto Research Chemicals (Toronto, Ontario, Canada). DHPN was obtained from Nacalai Tesque Inc. (Kyoto, Japan).

Animals

Female 5-week-old A/J mice were obtained from Japan SLC, Inc. (Shizuoka, Japan). Male 4-week-old F344 rats were purchased from Charles River Laboratories Japan, Inc. (Atsugi, Japan). Experimental animals were maintained at the Division of Animal Experiments of the Life Science Research Center at Kagawa University according to the institutional animal care guidelines. The regulations included the best considerations on animal welfare and good practice of animal handling contributing to the replacement, refinement, and reduction of animal testing (3Rs). The experimental protocol was approved by the Animal Care and Use Committee of Kagawa University. Animals were housed in polycarbonate cages with white wood chips for bedding under controlled conditions of humidity (60 ± 10%), lighting (12-h light/dark cycle), and temperature (24 ± 2°C) and had free access to drinking water and the basal diet (CE-2, CLEA Japan Inc., Tokyo, Japan).

Experimental design

The experimental designs are summarized in Table 1.

Experiment 1: Thirty-six 6-week-old female A/J mice were randomly divided into three groups (Groups 1 to 3) of 7, 14, and 15 rats, respectively. On Day 0 of the experiment, all mice in Groups 1, 2, and 3 underwent a left thoracotomy, with those of Groups 2 and 3 treated with 3 mg TISMO suspended in 0.2 mL saline per mouse administered directly into the left pleural cavity. Under deep anesthesia, a skin incision (approximately 7 mm long) was made on the left axilla. After confirmation of the location of the thoracic wall, a thoracotomy was completed with an incision (approximately 5 mm long) between the ribs. The left lung was observed directly through the opened hole, and atelectasis was confirmed. After infusion of the test solutions into the left pleural cavity, the skin was clipped together to close the thorax[10, 22]. Groups 1 and 3 were fed the basal diet mixed with AH at a dose of 120 ppm for 16 weeks. The concentration of AH was based on the human conventional dose of 45 mg/man/day[5], which corresponds to approximately 12 ppm in diet for mice and rats. Each mouse was euthanized by exsanguination from the abdominal aorta and postcava with a disposable syringe and needle under deep anesthesia at Week 16. After euthanization, the mice were subjected to autopsy.

Experiment 2: Forty-four 6-week-old female A/J mice were randomly divided into three groups (Groups 1, 2, and 3) of 15, 14, and 15 rats, respectively. The mice received an intraperitoneal (i.p.) administration of NNK (2 mg/0.1 ml saline/mouse) once weekly for 2 weeks (two treatments in total). AH was administered in the basal diet to Groups 2 and 3 at doses of 12 and 120 ppm, respectively, for 16 weeks. Each mouse was euthanized by exsanguination from the abdominal aorta and postcava with a disposable syringe and needle under deep anesthesia at Week 16. After euthanization, the mice were subjected to autopsy.

Experiment 3: Fifty-one 6-week-old male F344 rats were randomly divided into four groups (Groups 1 to 4). Group 1 was composed of 6 rats, and Groups 2, 3, and 4 were composed of 15 rats each. AH was administered to Group 1 at doses of 120 ppm from Weeks 2 to 30. Groups 2,

Table 1. Experimental Design (Experiments 1–3)

Group	Species	Gender[a]	Treatment[b]	Duration[c]	No.[d]
Experiment 1					
1	A/J mouse	F	120 ppm AH	16	7
2	A/J mouse	F	TISMO	16	14
3	A/J mouse	F	TISMO + 120 ppm AH	16	15
Experiment 2					
1	A/J mouse	F	NNK	16	15
2	A/J mouse	F	NNK + 12 ppm AH	16	14
3	A/J mouse	F	NNK + 120 ppm AH	16	15
Experiment 3					
1	F344 rat	M	120 ppm AH	30	6
2	F344 rat	M	DHPN	30	15
3	F344 rat	M	DHPN + 12 ppm AH	30	15
4	F344 rat	M	DHPN + 120 ppm AH	30	15

[a]F, female; M, male. [b]TISMO was intrathoracically infused at 3 mg/0.2 mL/mouse once; NNK was i.p. administered at 2 mg/0.1 mL saline/mouse twice; and 0.1% DHPN was administered in drinking water for 2 weeks. [c]Weeks. [d]Number of animals.

3, and 4 received 0.1% DHPN in drinking water for 2 weeks followed by the administration of AH in the basal diet at concentrations of 0, 12, and 120 ppm, respectively, for 28 weeks. Each rat was euthanized by exsanguination from the abdominal aorta and postcava with a disposable syringe and needle under deep anesthesia at Week 30. After euthanization, the rats were subjected to autopsy.

Body weight measurement, hematology, and plasma biochemistry

All rats and mice were weighed once weekly. For 2–7 mice in all groups in experiment 1 and all rats in experiment 3, hematological analysis was conducted at the beginning of autopsy. In addition, plasma biochemistry analysis was performed for 4–7 mice in all groups in experiment 1, 13 or 14 mice in all groups in experiment 2, and all rats in experiment 3. Each animal was laparotomized under deep anesthesia and euthanized by exsanguination from the abdominal aorta and postcava with a disposable syringe and needle on the day of autopsy. The collected blood in the syringe was dispensed into two test tubes containing an anticoagulant. Whole blood in one test tube was subjected to hematological analysis, while plasma obtained by the centrifugation of blood in the other test tube was used for plasma biochemistry testing. The examined hematological parameters were white blood cell (WBC) counts, red blood cell (RBC) counts, hemoglobin, hematocrit, mean corpuscular volume (MCV), mean corpuscular hemoglobin (MCH), mean corpuscular hemoglobin concentration (MCHC), platelets, and differential WBC counts (percentage and counts of stab neutrophils, segmented neutrophils, lymphocytes, monocytes, eosinophils and basophils). The examined plasma biochemistry parameters were aspartate aminotransferase (AST), alanine aminotransferase (ALT), lactate dehydrogenase (LDH), alkaline phosphatase (ALP), γ-glutamyl transpeptidase (γ-GTP), total bilirubin (T-Bil), glucose (Glu), total cholesterol (T-Chol), triglyceride (TG), total protein (TP), albumin (Alb), albumin-globulin ratio

(A/G); blood urea nitrogen (BUN), creatinine (Cre), sodium (Na), chloride (Cl), potassium (K), calcium (Ca), and inorganic phosphorus (IP).

Tissue preparation

At autopsy, the lungs, trachea, and heart were removed; 10% phosphate-buffered formalin was infused through the trachea, and the samples were rinsed and immersed in the fixative. Lung tissues were routinely embedded in paraffin, sectioned, and stained with hematoxylin and eosin (H.E.) for histopathological examination.

Macroscopic and histopathological analysis

Experiment 1: Pleural and alveolar findings, including the incidence of pleural thickening due to foreign body granuloma with infused fibers, pleural thickening mainly due to lymphocyte infiltration, lymphocyte infiltration in interstitium, lymphocytic foci, and macrophage and neutrophil infiltration in alveoli, were histopathologically determined in Groups 1, 2, and 3. The values of the thickest part of the pleura throughout all lung lobes were measured for each animal in Groups 2 and 3 using a virtual slide scan system (NanoZoomer 2.0-HT, Hamamatsu Photonics K.K., Shizuoka, Japan). Immunohistochemistry, from deparaffinization to counterstaining with hematoxylin, was performed automatically using a Ventana Discovery™ staining system (Ventana Medical Systems, Tucson, AZ, USA). RiboCC solution (Ventana Medical Systems, Tucson, AZ, USA) and CC1 solution (Ventana Medical Systems) were used for antigen retrieval. The primary antibodies were anti-tumor necrosis factor alpha (TNF-α) (ab6671, rabbit polyclonal antibody, Abcam, Cambridge, England) (diluted at 1:100 and 1:500), anti-interleukin 1 beta (IL-1β) (ab9722, rabbit polyclonal antibody, Abcam) (diluted at 1:100), anti-interleukin 6 (IL-6) (ab7737, rabbit polyclonal antibody, Abcam) (diluted at 1:50, 1:100, and 1:500), and anti-CD68 (ab125212, rabbit polyclonal antibody, Abcam) (diluted at 1:50). The expressions for each marker were evaluated as negative (–), weakly

positive (+), or strongly positive (++).

Experiment 2: After fixation in formalin, gross inspection of lungs was performed with a stereomicroscope. All macroscopically detected lung nodules were counted and trimmed for histopathological evaluation. Each lung lobe of all the mice was examined histopathologically. Proliferative lung lesions were diagnosed as bronchioloalveolar hyperplasia (hyperplasia), bronchioloalveolar adenoma (adenoma), or bronchioloalveolar carcinoma (adenocarcinoma) according to the criteria of the International Harmonization of Nomenclature and Diagnostic Criteria (INHAND)[23]. The multiplicities of proliferative lung lesions were microscopically counted on H.E. sections. Areas of adenoma regions were measured using a NanoZoomer 2.0-HT.

Experiment 3: Lung lesions from the rat DHPN-induced lung carcinogenesis model were categorized as hyperplasia, adenoma, or adenocarcinoma, as in Experiment 2 and following the established criteria in INHAND[23]. The multiplicities of neoplastic lung lesions, adenomas, and adenocarcinomas were counted on H.E. sections with a light microscope. Although many hyperplasias were observed in rats treated with DHPN, they were not counted because hyperplasias induced by DHPN in F344 rats tend to grow and merge with each other.

Statistical analysis

Means and standard deviations (S.D.) were calculated from quantitative data for body weights, hematological tests, plasma biochemistry tests, multiplicities and areas of proliferative lung lesions, and maximum pleural thickness. Data are expressed as the mean ± S.D. A statistical analysis system (EXSUS version 8.0, CAC Croit Corporation, Tokyo, Japan) was used for the statistical analyses of all experimental data. Levels of p<0.05 were established as the significance levels for each statistical test.

Experiment 1: Incidences of histopathological findings were analyzed by Fisher's exact test. Body weight, plasma biochemistry parameters, and pleural thickness were analyzed by Tukey-type multiple comparison test. Group 2 was selected as the reference group for the statistical analysis of hematology in Group 3 by F-test because there were not three or more mice in Group 1 from which sufficient blood volumes could be collected for hematology due to a technical error on our part. When the data in each group were homogenous, a parametric Student's t-test was performed. When the data in each group were heterogeneous, Aspin–Welch's t-test was performed.

Experiments 2 and 3: Incidences of histopathological proliferative lesions were analyzed by Fisher's exact test. Body weight, hematology, plasma biochemistry, multiplicities of gross nodules and histopathological proliferative lesions, and area of the adenoma were analyzed by Tukey-type multiple comparison test.

Results

Experiment 1

Body weight: Growth curves for each group are shown in Fig. 1. Body weights in the TISMO-treated groups (Groups 2 and 3) showed a significant decrease from 2 weeks after administration compared with those in the TISMO-untreated group (Group 1). The body weights of Groups 2 and 3 mice demonstrated similar trends until Week 9. However, the body weights of mice in Group 3 (TISMO + 120 ppm AH-treated group) recovered from Week 10 to levels similar to that of mice in Group 1 (120 ppm AH-treated group) at Week 12. Furthermore, the body weights of Group 3 mice completely recovered and were significantly higher than those of Group 2 (TISMO-treated group) mice from Week 13 to 14, and their body weight values also showed a tendency to be higher than those of mice in Group 2 from Weeks 15 to the end of the experiment (Week 16).

Hematology and plasma biochemistry: In hematological analysis, the mice in Group 3 showed a significant decrease in white blood cell counts compared with those in Group 2 (Fig. 2). In plasma biochemistry, no differences
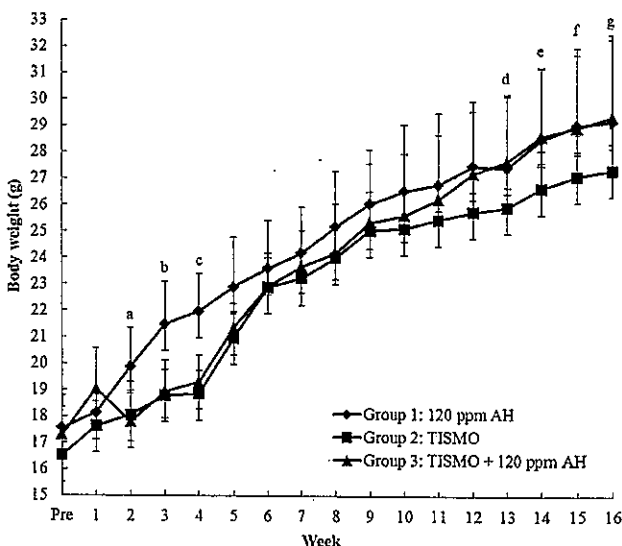
Fig. 1. Body weights of A/J mice in experiment 1. A significant decrease in body weight was observed in the TISMO-treated groups (Groups 2 and 3) compared with the untreated group (Group 1) from 2 weeks after TISMO administration. Significantly different from Group 1 at (a) p<0.05 (Groups 2 and 3 vs. Group 1), (b) p<0.01 (Groups 2 and 3 vs. Group 1), and (c) p<0.001 (Group 2 vs. Group 1) and p<0.01 (Group 3 vs. Group 1). However, the mice in Group 3 (TISMO + 120 ppm AH-treated group) showed recovery of body weight, and they showed significantly higher body weight values than those of mice in Group 2 (TISMO-treated group) from Weeks 13 to 14. Their body weight values also showed a tendency to be higher than those of mice in Group 2 from Weeks 15 to 16. Significantly different from Group 2 at (d, e) p<0.05 (Group 3 vs. Group 2), (f) p=0.09 (Group 3 vs. Group 2), and (g) p=0.07 (Group 3 vs. Group 2).

were observed with respect to TISMO or AH treatment (data not shown).

Histopathological analyses: At autopsy, portions of lung lobes showed marked adhesion to other lobes in the TISMO-treated groups (Groups 2 and 3). The incidence of inflammatory lesions in the lung is summarized in Table 2. Pleural thickening and inflammation were found in all mice in these groups. Pleural thickening lesions were due to foreign body granuloma with infused TISMO fibers, which were histopathologically observed as brown fine fibers in Groups 2 and 3 (Fig. 3a). In the lesions, TISMO fibers accumulated inside the cytoplasm of multiple macrophages and
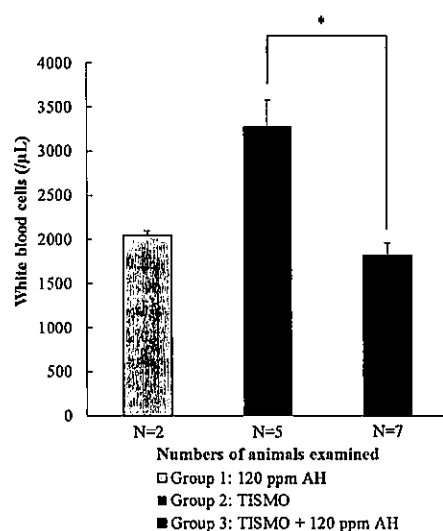
foreign-body giant cells (Fig. 3b). Although there was no statistically significant difference in the incidence of lesions between Groups 2 and 3, Group 3 tended toward a lower incidence than Group 2 (Table 2, p=0.08). Pleural thickening lesions mainly caused by lymphocytic infiltration were also observed in the same groups (Fig. 3c). There were no significant differences in the incidence of lesions between Groups 2 and 3. Lymphocyte infiltration in the interstitium, which was considered attributable to TISMO treatment, was observed in only one mouse in Group 2 (Fig. 3d). Lymphocytic foci (Fig. 3e) and macrophage and neutrophil infiltration in alveoli (figure not shown) were observed in Groups 2 and 3 and also in Group 1 (TISMO-untreated group). These findings were not considered related to TISMO infusion because no significant differences were observed in any of the groups.

The thickness of the thickest part of the pleura in Group 3 was significantly higher than that in Group 1. However, no significant difference from the data of Group 2 was noted (Table 2).

Macrophages and foreign body giant cells in the pleurae (Fig. 4a) and in alveoli (Fig. 4b) showed strongly positive for CD68 immunohistochemically. These CD68-positive cells in alveoli were especially noted to be located closed to the thickening pleurae. In addition, macrophages and foreign body giant cells in pleurae were weakly positive (Fig. 4c), and macrophages in alveoli were weakly or strongly positive for IL-1β (Fig. 4d). These IL-1β-positive cells approximately corresponded to CD68-positive cells. However, no apparent differences between AH treatment and lack of treatment were observed immunohistochemically in the expression of IL-1β. Lymphocytes in the pleurae and lymphocytic foci were negative both for CD68 and IL-1β. In addition, no cells positive for TNF-α and IL-6 were detected under several conditions of antigen retrieval and antibody dilution that were selected in the present study.

Fig. 2. White blood cell counts in experiment 1. A significant decrease in white blood cell counts was observed in Group 3 (TISMO + 120 ppm AH-treated group) compared with Group 2 (TISMO-treated group). *Significantly different from Group 2 at p<0.05.

Table 2. Incidences of Histopathological Findings in the Lung and Values of the Thickest Part of the Pleura (Experiment 1)

Group	1	2	3
Treatment	120 ppm AH	TISMO	TISMO + 120 ppm AH
No.[a]	7	14	15
1. Incidence of histopathological findings	Incidence (%)		
1.1 Pleura			
Thickening due to foreign body granuloma with infused fibers	0/7 (0.0)	11/14 (78.6)	7/15 (46.7)[b]
Thickening mainly due to lymphocyte infiltration	0/7 (0.0)	14/14 (100.0)	14/15 (93.3)[c]
1.2 Lung parenchyma			
Lymphocyte infiltration in interstitium	0/7 (0.0)	1/14 (7.1)	0/15 (0.0)
Lymphocytic foci	2/7 (28.6)	8/14 (57.1)	6/15 (40.0)
Macrophage and neutrophil infiltration in alveoli	1/7 (14.3)	1/14 (7.1)	2/15 (13.3)
2. Values of the thickest part of the pleura	Pleural thickness[d]		
	4.9 ± 0.9	90.6 ± 36.3[e]	99.7 ± 26.9[f]

[a]Number of mice. [b]Significantly different from Group 1 by Fisher's exact test at p<0.05; no significantly difference from Group 2 but a tendency toward a decrease by Fisher's exact test (p=0.08). [c]Significantly different from Group 1 by Fisher's exact test at p<0.01. [d]Micrometers, mean ± standard deviation. [e, f]Significantly different from Group 1 by Tukey-type multiple comparison test at p<0.01 and p<0.001, respectively.
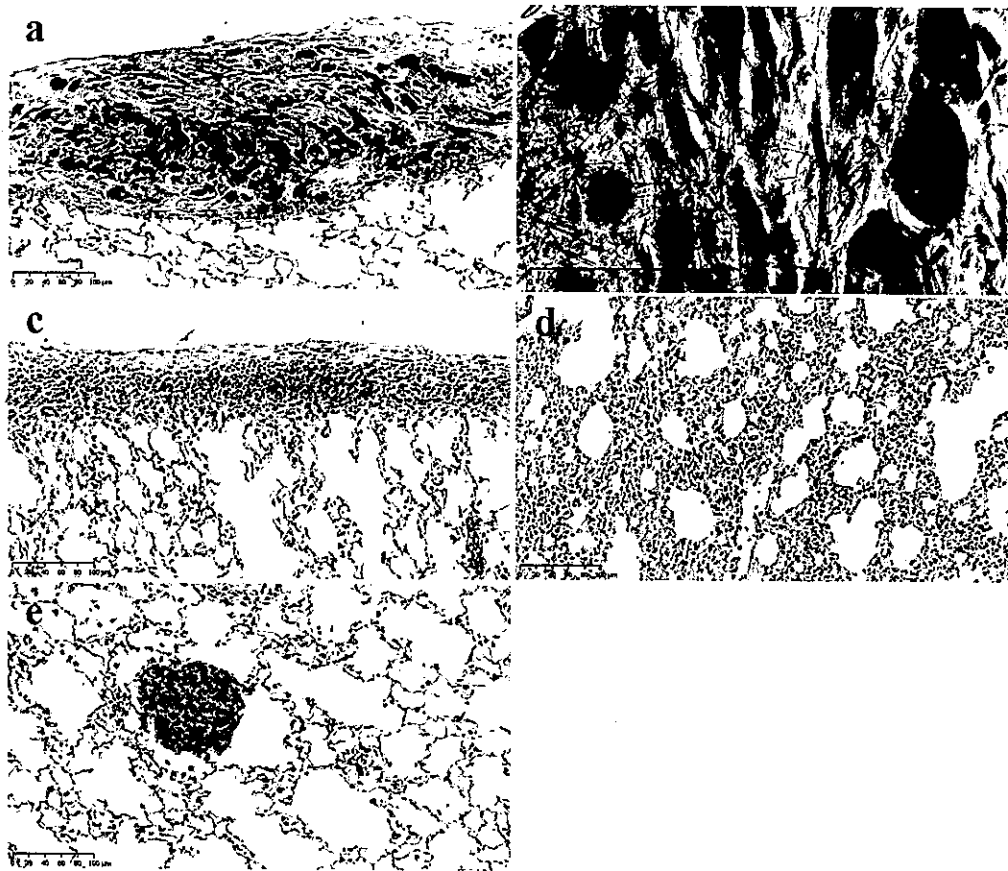
Fig. 3. Histopathological findings in the TISMO-treated groups (Groups 1, 2, and 3) in experiment 1. Bar = 100 μm except in (b). Bar = 50 μm in (b). (a) Pleural thickening due to foreign body granuloma with infused fibers, (b) accumulation of TISMO fibers in cytoplasm of macrophages and foreign-body giant cells, (c) pleural thickening primarily due to infiltrated lymphocytes, (d) lymphocyte infiltration in the interstitium, and (e) lymphocytic foci in the interstitium.

Table 3. Multiplicities of Macroscopic Nodules, Incidences and Multiplicities of Microscopic Lung Nodules, and Areas of Adenomas (Experiment 2)

| Group	Treatment	No.[a]	Macroscopy[b] Multiplicity of macroscopic nodules[c]	Histopathology Incidence (%) Hyperplasia	Adenoma	Adenocarcinoma	Multiplicity[c] Hyperplasia	Adenoma	Adenocarcinoma	Area of adenoma[d]
1	NNK	15	29.7 ± 11.0	15/15 (100.0)	15/15 (100.0)	0/15 (0.0)	9.6 ± 5.8	11.3 ± 6.0	0.0 ± 0.0	0.2 ± 0.1
2	NNK + 12 ppm AH	14	33.8 ± 14.9	14/14 (100.0)	14/14 (100.0)	1/14 (7.1)	14.3 ± 7.1	20.4 ± 10.3*	0.1 ± 0.3	0.2 ± 0.1
3	NNK + 120 ppm AH	15	28.4 ± 13.4	15/15 (100.0)	15/15 (100.0)	0/15 (0.0)	10.7 ± 5.5	12.6 ± 5.1	0.0 ± 0.0	0.3 ± 0.1

[a]Number of mice. [b]Gross inspection with a stereomicroscope. [c]Mean ± standard deviation. [d]Square millimeters. *Significantly different from Group 1 by Tukey-type multiple comparison test at $p < 0.05$.

Experiment 2

Body weight and plasma biochemistry: No significant variations in body weight or plasma biochemistry were observed, regardless of AH treatment (data not shown).

Macroscopic and histopathological analyses: Using a stereomicroscope, white nodules were detected in the lungs of all mice. However, no significant difference was noted in the multiplicities of gross nodules regardless of AH treat-

ment or AH concentrations (Table 3). Histopathologically, hyperplasias (Fig. 5a), adenomas (Fig. 5c), and adenocarcinomas (Fig. 5d) were observed in the lungs of all NNK-treated groups (Groups 1, 2, and 3). The incidences and multiplicities of lung lesions are summarized in Table 3. With respect to incidence, no significant differences were observed in the AH-treated groups (Groups 2 and 3) compared with the AH-untreated group (Group 1). Adenoma
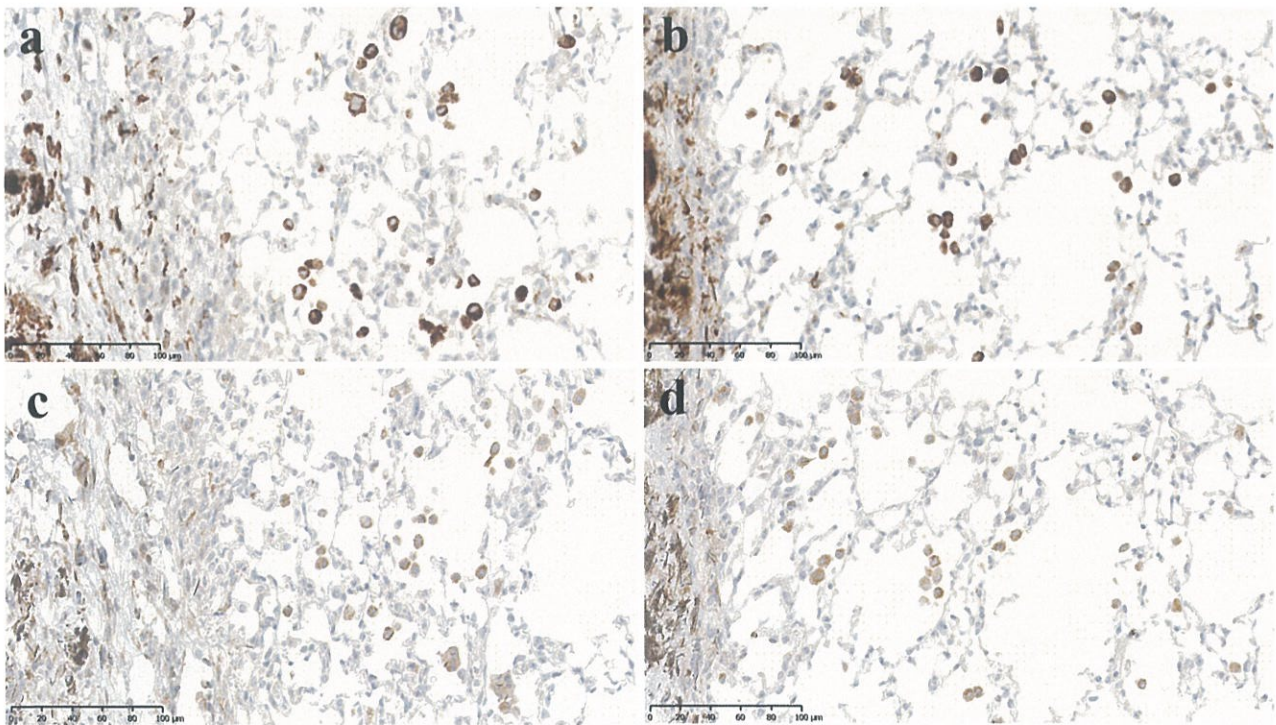
Fig. 4. Immunohistochemical findings for macrophages in alveoli of a lung peripheral lesion adjacent to granulation tissues in experiment 1. Bar = 100 μm. (a) Strongly positivity (++) for CD68 in Group 2, (b) strongly positivity (++) for CD68 in Group 3, (c) weakly positivity (+) for IL-1β in Group 2, and (d) weakly positivity (+) for IL-1β in Group 3.

multiplicity in Group 2 (NNK + 12 ppm AH-treated group) showed a significant increase compared with that in Group 1 (NNK-treated group). However, Group 3 (NNK + 120 ppm AH-treated group) did not show any significant increase in the multiplicities of proliferative lesions as compared with Group 1. Regarding the areas of the adenomas, no significant differences were observed in Groups 1, 2, and 3 (Table 3).

Experiment 3

Body weight: The body weights of rats in Groups 2, 3, and 4 (DHPN + 0, 12 or 120 ppm AH-treated groups, respectively) significantly decreased compared with those of rats in Group 1 (120 ppm AH-treated group) (Fig. 6). Groups 3 and 4 showed a similar trend to Group 2. However, there was no significant variation among Groups 2, 3, and 4.

Hematology and plasma biochemistry: In hematological and plasma biochemistry analyses, no changes related to treatment with DHPN or AH were observed in any group (data not shown).

Histopathological analyses: Hyperplasias (Fig. 5b), adenomas (Fig. 5d), and adenocarcinomas (Fig. 5e) were observed in the lungs of the DHPN-treated groups (Groups 2, 3, and 4). Regarding the incidences and multiplicities of each type of lung proliferative lesions, no significant differences were observed in the AH-treated groups (Groups 3 and 4) compared with the AH-untreated group (Group 2) (Table 4). Furthermore, no differences attributable to AH concentration were observed in Groups 3 and 4.

Discussion

The present study showed that AH significantly remedied body weight gain and decreased white blood cell counts in a mouse model of TISMO-induced pleural thickening. TISMO intrathoracic infusion induced pleural thickening in A/J mice, as shown in our previous study[10]. AH was therefore expected to induce a suppressive effect on pleural thickening caused by TISMO infusion. In our previous studies, experiments using rodent models of TISMO-induced pleural lesions imitating pleural mesothelioma were conducted to support the development of treatment modalities for malignant mesothelioma, for which an appropriate animal model is required[10, 22, 24]. Fiber-shaped particles such as asbestos have iron as a component and also generate free radicals[25]. Although TISMO contains no iron, the TISMO fibers produced a severe reaction, and the accumulation of iron was observed around the infused TISMO fibers using Berlin blue staining in our previous study[10]. Thus, iron accumulation was likely to have derived from an endogenous source in the body[10]. Iron increases oxidant stress, leads to thickening and inflammation of pleurae, and has a potential role in underlying carcinogenic mechanisms[25, 26].

In experiment 1, all mice treated with TISMO (Groups 2 and 3) showed histopathological pleural thickening with severe chronic inflammatory changes. In Group 2 (TISMO-treated group), TISMO treatment also appeared to induce an increase in peripheral white blood cell counts caused
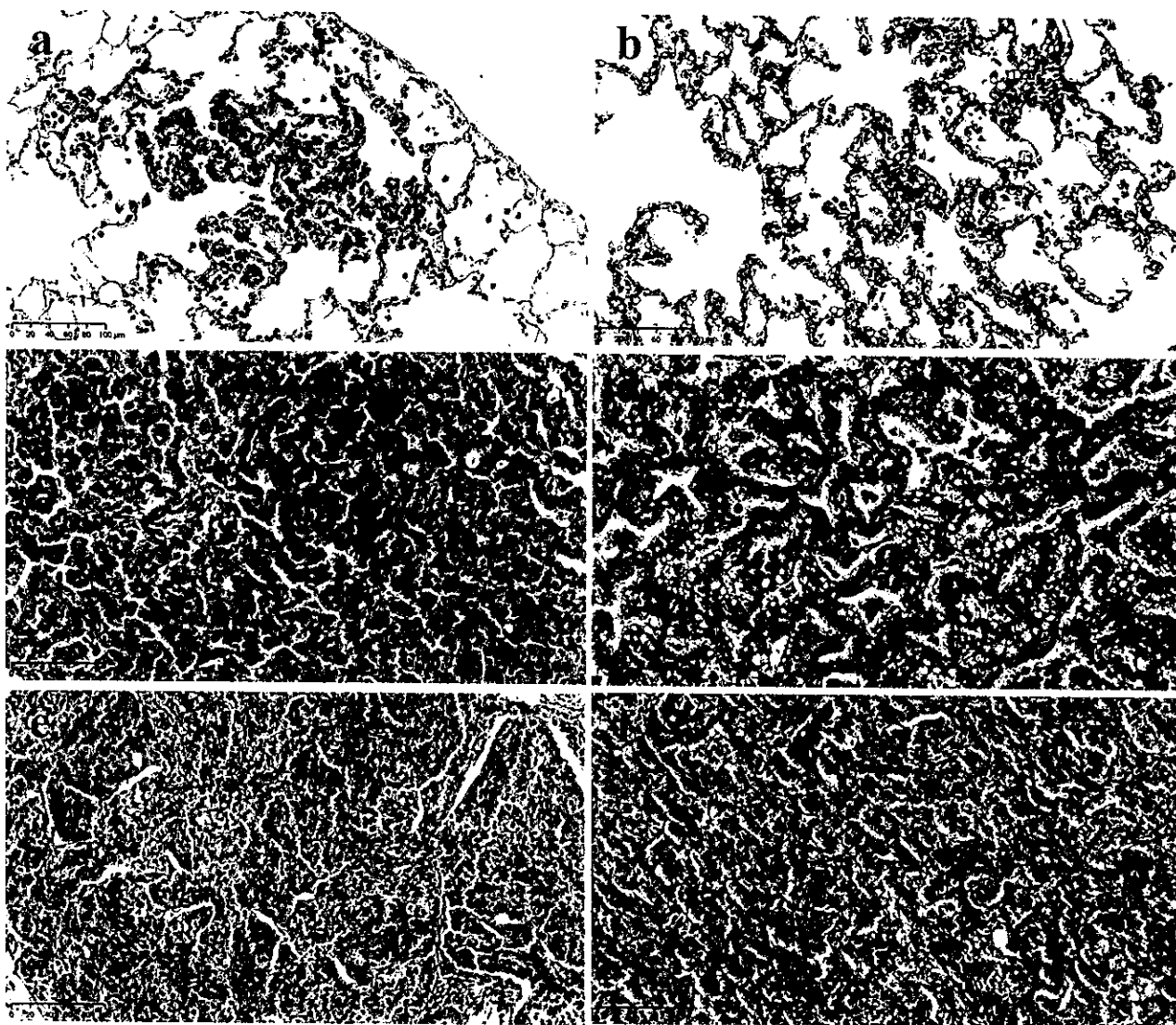
Fig. 5. Histopathological findings in proliferative lesions in experiment 2 and 3 (hematoxylin and eosin staining). Bar = 100 μm. (a, c, e) Lesions induced by NNK can be seen in the A/J mouse lung. (b, d, f) Lesions induced by DHPN can be seen in the F344 rat lung. (a, b) Bronchioloalveolar hyperplasia, (c, d) bronchioloalveolar adenoma, and (e, f) bronchioloalveolar carcinoma.
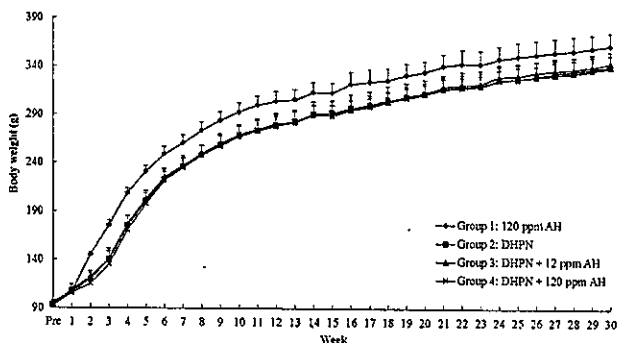

Fig. 6. Body weights of F344 rats in experiment 3. Body weights in Groups 2, 3, and 4 (DHPN + 0, 12, or 120 ppm AH-treated groups, respectively) significantly decreased compared with those in Group 1 (120 ppm AH-treated group) from Week 2 to the end of the experiment (Week 30).

by inflammation. In addition, the TISMO-treated groups had lower body weights than the TISMO-untreated group (Group 1) after TISMO administration, likely because of the poor general conditions of the animals arising from acute inflammation. The mice in Group 3 (TISMO + 120 ppm AH-treated group) showed a trend toward body weight recovery from Week 10 and demonstrated completely recovery of body weight at Week 13. The recovery of body weight in Group 3 appeared to be attributable to an improvement in the poor general condition caused by TISMO because of the effect of AH on inflammatory suppression. Furthermore, mice in Group 3 (TISMO + 120 ppm AH-treated group) showed an apparent recovery in white blood cell counts, reaching the same levels as mice in the TISMO-untreated group (Group 1). These results suggest that AH exerted a suppressive effect on inflammation, at least with respect to

Table 4. Incidences and Multiplicities of Histopathological Lung Nodules (Experiment 3)

Group	Treatment	No.[a]	Incidence (%)			Multiplicity[b]	
			Hyperplasia	Adenoma	Adenocarcinoma	Adenoma	Adenocarcinoma
1	120 ppm AH	6	0/6 (0.0)	0/6 (0.0)	0/6 (0.0)	0.0 ± 0.0	0.0 ± 0.0
2	DHPN	15	15/15 (100.0)	15/15 (100.0)	5/15 (33.3)	3.5 ± 2.2	0.3 ± 0.5
3	DHPN + 12 ppm AH	15	15/15 (100.0)	15/15 (100.0)	4/15 (26.7)	4.3 ± 2.1	0.5 ± 1.1
4	DHPN + 120 ppm AH	15	15/15 (100.0)	15/15 (100.0)	7/15 (46.7)	4.0 ± 1.9	0.6 ± 0.8

[a]Number of rats. [b]Mean ± standard deviation. The multiplicities of hyperplasias were not counted (see main text).

the increase in peripheral white blood cells induced by the intrathoracic administration of TISMO.

Pleural thickening was caused mainly by foreign body granuloma with infused fiber, infiltrated lymphocytes, and fibrosis. Although this histopathological finding was noted both in Groups 2 and 3, no significant difference in histopathological incidence of inflammatory lesions and pleural thickness was observed between Groups 2 and 3, regardless of AH treatment. However, a suppressive effect of AH was demonstrated histopathologically on quartz-induced lung inflammation in our previous study[9]. These results indicates that the suppressive effects of AH administration on lung inflammation might be observed in the lung parenchyma, not in the pleura, assuming that increased levels of SPs contribute to the suppressive mechanism. On the other hand, no significant changes were observed in SP-B and SP-C expression following AH treatment in our previous study[9]. Therefore, the suppressive effects of AH on lung inflammation might be exerted via mechanisms other than increasing SPs, such as effects on excretion and other processes[27, 28]. In fact, pleural thickening attributable to foreign body granuloma with infused TISMO tended to be decreased in Group 3 compared with Group 2 in this study, indicating that AH had the potential to excrete biological foreign bodies. TISMO fibers accumulated inside the cytoplasm of macrophages and foreign-body giant cells, likely having been phagocytized by these cells, and remained in place for prolonged periods. Indirect effects of fibers such as the inhibition of phagocytosis by macrophages have been proposed as a candidate mechanism for fiber-induced carcinogenesis[29]. Long multiwall carbon nanotubes (MWCNTs) and long asbestos fibers induce frustrated phagocytosis and granuloma formation[30]. Determination of a strategy for the removal of MWCNTs, asbestos, and TISMO may contribute to the prevention of mesothelioma carcinogenesis.

The decrease in white blood cell counts in peripheral blood was considered attributable to AH inhibiting inflammatory mediators or oxidative stress released by TISMO. In rats with paraquat-induced lung fibrosis, the protective effect of ambroxol was histologically prominent and presumably mediated by its free radical scavenging and antioxidant activity[8]. AH has also been reported to suppress the lipopolysaccharide-induced production of TNF-α, IL-1β, IL-6, and reactive oxygen species in macrophages derived from rats *in vitro*[31]. CD68, which is marker of macrophage was chosen to confirm producer cells of these cytokines in

the present experiment. However, there was no apparent difference in the expression of IL-1β, at least in the lung considering the results of immunohistochemistry. Therefore, AH might affect other mediators than IL-1β *in vivo* or have effects on mediators in the peripheral blood. In this experiment, TNF-α and IL-6-expressing cells were not able to be detected in the lung. One of the reasons for this is known to be that it is generally difficult to detect cytokines in a paraffinized specimen by immunohistochemistry because they are immediately secreted from their producer cells after synthesis[32, 33].

Both NNK and DHPN are known lung carcinogens. All mice and rats showed adenoma formation in experiments 2 and 3, and adenocarcinomas were also observed in several animals. In our previous experiment, SP-B and SP-C were highly expressed in lung hyperplasias and adenomas induced by DHPN in male F344 rats[2]. Thus, SPs were expected to be associated with lung tumorigenesis. Adenoma multiplicity in Group 2 (NNK + 12 ppm AH-treated group) showed a significant increase compared with that in Group 1 (NNK-treated group), although Group 3 (NNK + 120 ppm AH-treated group) did not show any significant increase in the multiplicities of proliferative lesions as compared with Group 1. The increased adenomas were considered to have occurred incidentally, as there was no AH-concentration dependency. Therefore, in the present study, no significant changes related to AH treatment were observed in the incidence and multiplicity of proliferative lung lesions. These results suggested that SPs did not appear to exert a directly modulatory effect on proliferative lung lesions. SPs highly expressed in lung tumors in our previous study may have been the result of proliferation of type II alveolar epithelial cells producing SPs physiologically and may not have been related to the lung tumorigenesis.

In conclusion, AH suppressed TISMO-induced inflammation and was associated with recovery of body weight loss and decreased peripheral white blood cell counts. However, modulatory effects on proliferative lung lesions induced by NNK and DHPN were not identified in the present study. Thus, these results suggest that AH potentially exerts anti-inflammatory effects but does not have a direct suppressive effect on lung tumorigenesis in rodents.

Disclosure of Potential Conflicts of Interest: The authors declare that there are no conflicts of interest associated with this manuscript.

References

1. Pérez-Gil J, and Keough KM. Interfacial properties of surfactant proteins. Biochim Biophys Acta. **1408**: 203–217. 1998. [Medline] [CrossRef]

2. Yokohira M, Yamakawa K, Nakano Y, Numano T, Furukawa F, Kishi S, Ninomiya F, Kanie S, Hitotsumachi H, Saoo K, and Imaida K. Immunohistochemical characteristics of surfactant proteins a, B, C and d in inflammatory and tumorigenic lung lesions of f344 rats. J Toxicol Pathol. **27**: 175–182. 2014. [Medline] [CrossRef]

3. Yokohira M, Kuno T, Yamakawa K, Hashimoto N, Ninomiya F, Suzuki S, Saoo K, and Imaida K. An intratracheal instillation bioassay system for detection of lung toxicity due to fine particles in f344 rats. J Toxicol Pathol. **22**: 1–10. 2009. [Medline] [CrossRef]

4. Houtmeyers E, Gosselink R, Gayan-Ramirez G, and Decramer M. Effects of drugs on mucus clearance. Eur Respir J. **14**: 452–467. 1999. [Medline] [CrossRef]

5. Nagahama FN, Momose T, Ogiwara M, Suetsugu S, Umeda H, Kawai M, Maekawa N, Inaba N, Oda Y, Uchihira F, Konishiike J, Sera Y, Ooka Y, Oishi M, Nakajima S, Sewake N, Mochizuki K, Kodomari N, Inoue K, Tsurutani H, and Nagano H. Efficacy and safety of long-term treatment with mucolytic agent (NA872) in chronic respiratory disease patients. Yakuri To Chiryo. **9**: 2091–2104. 1981; (Japanese Pharmacology and Therapeutics).

6. Seifart C, Clostermann U, Seifart U, Müller B, Vogelmeier C, von Wichert P, and Fehrenbach H. Cell-specific modulation of surfactant proteins by ambroxol treatment. Toxicol Appl Pharmacol. **203**: 27–35. 2005. [Medline] [CrossRef]

7. Gao X, Huang Y, Han Y, Bai CX, and Wang G. The protective effects of Ambroxol in Pseudomonas aeruginosa-induced pneumonia in rats. Arch Med Sci. **7**: 405–413. 2011. [Medline] [CrossRef]

8. Zhi QM, Yang LT, and Sun HC. Protective effect of ambroxol against paraquat-induced pulmonary fibrosis in rats. Intern Med. **50**: 1879–1887. 2011. [Medline] [CrossRef]

9. Kanie S, Yokohira M, Yamakawa K, Nakano-Narusawa Y, Yoshida S, Hashimoto N, and Imaida K. Suppressive effects of the expectorant drug ambroxol hydrochloride on quartz-induced lung inflammation in F344 rats. J Toxicol Pathol. **30**: 153–159. 2017. [Medline] [CrossRef]

10. Yokohira M, Hashimoto N, Yamakawa K, Suzuki S, Saoo K, Kuno T, and Imaida K. Potassium octatitanate fibers (TISMO) induce pleural mesothelial cell reactions with iron accumulation in female A/J mice. Oncol Lett. **1**: 589–594. 2010. [Medline] [CrossRef]

11. Akopyan G, and Bonavida B. Understanding tobacco smoke carcinogen NNK and lung tumorigenesis. Int J Oncol. **29**: 745–752. 2006. [Medline]

12. Chen RJ, Chang LW, Lin P, and Wang YJ. Epigenetic effects and molecular mechanisms of tumorigenesis induced by cigarette smoke: an overview. J Oncol. **2011**: 654931. 2011. [Medline] [CrossRef]

13. Belinsky SA, Devereux TR, Foley JF, Maronpot RR, and Anderson MW. Role of the alveolar type II cell in the development and progression of pulmonary tumors induced by 4-(methylnitrosamino)-1-(3-pyridyl)-1-butanone in the A/J mouse. Cancer Res. **52**: 3164–3173. 1992. [Medline]

14. Igarashi M, Watanabe M, Yoshida M, Sugaya K, Endo Y, Miyajima N, Abe M, Sugano S, and Nakae D. Enhancement of lung carcinogenesis initiated with 4-(N-hydroxymethylnitrosamino)-1-(3-pyridyl)-1-butanone by Ogg1 gene deficiency in female, but not male, mice. J Toxicol Sci. **34**: 163–174. 2009. [Medline] [CrossRef]

15. Peterson LA, and Hecht SS. O6-methylguanine is a critical determinant of 4-(methylnitrosamino)-1-(3-pyridyl)-1-butanone tumorigenesis in A/J mouse lung. Cancer Res. **51**: 5557–5564. 1991. [Medline]

16. Fukuyama Y, Mitsudomi T, Sugio K, Ishida T, Akazawa K, and Sugimachi K. K-ras and p53 mutations are an independent unfavourable prognostic indicator in patients with non-small-cell lung cancer. Br J Cancer. **75**: 1125–1130. 1997. [Medline] [CrossRef]

17. Ronai ZA, Gradia S, Peterson LA, and Hecht SS. G to A transitions and G to T transversions in codon 12 of the Ki-ras oncogene isolated from mouse lung tumors induced by 4-(methylnitrosamino)-1-(3-pyridyl)-1-butanone (NNK) and related DNA methylating and pyridyloxobutylating agents. Carcinogenesis. **14**: 2419–2422. 1993. [Medline] [CrossRef]

18. Kitahashi T, Takahashi M, Yamada Y, Oghiso Y, Yokohira M, Imaida K, Tsutsumi M, Takasuka N, Sugimura T, and Wakabayashi K. Occurrence of mutations in the epidermal growth factor receptor gene in X-ray-induced rat lung tumors. Cancer Sci. **99**: 241–245. 2008. [Medline] [CrossRef]

19. Yamakawa K, Kuno T, Hashimoto N, Yokohira M, Suzuki S, Nakano Y, Saoo K, and Imaida K. Molecular analysis of carcinogen-induced rodent lung tumors: Involvement of microRNA expression and Kras or Egfr mutations. Mol Med Rep. **3**: 141–147. 2010. [Medline]

20. Yokohira M, Takeuchi H, Saoo K, Matsuda Y, Yamakawa K, Hosokawa K, Kuno T, and Imaida K. Establishment of a bioassay model for lung cancer chemoprevention initiated with 4-(methylnitrosamino)-1-(3-pyridyl)-1-butanone (NNK) in female A/J mice. Exp Toxicol Pathol. **60**: 469–473. 2008. [Medline] [CrossRef]

21. Yokohira M, Takeuchi H, Yamakawa K, Saoo K, Matsuda Y, Zeng Y, Hosokawa K, and Imaida K. Bioassay by intratracheal instillation for detection of lung toxicity due to fine particles in F344 male rats. Exp Toxicol Pathol. **58**: 211–221. 2007. [Medline] [CrossRef]

22. Yokohira M, Hashimoto N, Nakagawa T, Nakano Y, Yamakawa K, Kishi S, Kanie S, Ninomiya F, Saoo K, and Imaida K. Long-Term Chronic Toxicity and Mesothelial Cell Reactions Induced by Potassium Octatitanate Fibers (TISMO) in the Left Thoracic Cavity in A/J Female Mice. Int J Toxicol. **34**: 325–335. 2015. [Medline] [CrossRef]

23. Renne R, Brix A, Harkema J, Herbert R, Kittel B, Lewis D, March T, Nagano K, Pino M, Rittinghausen S, Rosenbruch M, Tellier P, and Wohrmann T. Proliferative and nonproliferative lesions of the rat and mouse respiratory tract. Toxicol Pathol. 37(Suppl): 5S–73S. 2009. [Medline] [CrossRef]

24. Yokohira M, Nakano-Narusawa Y, Yamakawa K, Hashimoto N, Yoshida S, Kanie S, and Imaida K. Chronic mesothelial reaction and toxicity of potassium octatitanate fibers in the pleural cavity in mice and F344 rats. Cancer Sci. **107**: 1047–1054. 2016. [Medline] [CrossRef]

25. Kamp DW, Graceffa P, Pryor WA, and Weitzman SA. The

role of free radicals in asbestos-induced diseases. Free Radic Biol Med. **12**: 293–315. 1992. [Medline] [CrossRef]

26. Toyokuni S. Elucidation of Asbestos-induced Carcinogenesis and Its Application to Prevention, Diagnosis and Treatment in Relation to Iron. Jpn J Lung Cancer. **49**: 362–367. 2009. [CrossRef]

27. Hosoe H, Kaise T, and Ohmori K. Erdosteine enhances mucociliary clearance in rats with and without airway inflammation. J Pharmacol Toxicol Methods. **40**: 165–171. 1998. [Medline] [CrossRef]

28. Ren YC, Wang L, He HB, and Tang X. Pulmonary selectivity and local pharmacokinetics of ambroxol hydrochloride dry powder inhalation in rat. J Pharm Sci. **98**: 1797–1803. 2009. [Medline] [CrossRef]

29. Dostert C, Pétrilli V, Van Bruggen R, Steele C, Mossman BT, and Tschopp J. Innate immune activation through Nalp3 inflammasome sensing of asbestos and silica. Science. **320**: 674–677. 2008. [Medline] [CrossRef]

30. Poland CA, Duffin R, Kinloch I, Maynard A, Wallace WA, Seaton A, Stone V, Brown S, Macnee W, and Donaldson K. Carbon nanotubes introduced into the abdominal cavity of mice show asbestos-like pathogenicity in a pilot study. Nat Nanotechnol. **3**: 423–428. 2008. [Medline] [CrossRef]

31. Jang YY, Song JH, Shin YK, Han ES, and Lee CS. Depressant effects of ambroxol and erdosteine on cytokine synthesis, granule enzyme release, and free radical production in rat alveolar macrophages activated by lipopolysaccharide. Pharmacol Toxicol. **92**: 173–179. 2003. [Medline] [CrossRef]

32. Furusu A, Miyazaki M, Koji T, Abe K, Ozono Y, Harada T, Nakane PK, Hara K, and Kohno S. Involvement of IL-4 in human glomerulonephritis: an in situ hybridization study of IL-4 mRNA and IL-4 receptor mRNA. J Am Soc Nephrol. **8**: 730–741. 1997. [Medline]

33. Tsutsumi H. Troubleshooting. In: Watanabe and Nakane's immunoenzymatic technique (Watanabe-Nakane Kouso-Koutai-Hou), 4 th ed. Nagura H., Nagamura Y., Tsutsumi H. (eds). Gakusai Kikaku, Tokyo, Japan. 335. 2002.